Shape coexistence in the transitional ^{133}Ba nucleus

S. Juutinen,[1] P. Šimeček,[2] P. Ahonen,[1] M. Carpenter,[3,*] C. Fahlander,[4] J. Gascon,[3,†] R. Julin,[1] A. Lampinen,[1] T. Lönnroth,[5] J. Nyberg,[3,4] A. Pakkanen,[1] M. Piiparinen,[1] K. Schiffer,[3] G. Sletten,[3] S. Törmänen,[1] and A. Virtanen[1]
[1]*Department of Physics, University of Jyväskylä, P.O. Box 35, FIN-40351 Jyväskylä, Finland*
[2]*Institute of Nuclear Physics, Czech Academy of Sciences, 250 68 Rez near Prag, Czech Republic*
[3]*The Niels Bohr Institute, Tandem Accelerator Laboratory, DK-4000 Roskilde, Denmark*
[4]*The Svedberg Laboratory, Uppsala University, Box 535, S-75121 Uppsala, Sweden*
[5]*Department of Physics, Åbo Akademi, FIN-20500 Turku, Finland*
(Received 13 September 1994)

High-spin states in the ^{133}Ba nucleus have been populated using the ^{124}Sn(^{13}C,4n) reaction. Excited states were observed up to I = 45/2 and several bands were constructed. Most of the observed bands are characterized by intense dipole transitions. At low spin, bands built on mixed $\nu s_{1/2}$ and $\nu d_{3/2}$ configurations and on the $\nu h_{11/2}$ configuration were observed. The latter band is associated with a large signature splitting of about 300 keV. According to total Routhian surface calculations, in this band the nucleus has a triaxial shape with $\gamma \approx$ -80°. At higher spin, bands built on three and five-quasiparticle configurations were identified. These bands may posses a weakly deformed shape with either γ>0° or γ<-60°, depending on the number of $h_{11/2}$ protons and neutrons involved in the configuration.

PACS number(s): 21.10.Re, 23.20.Lv, 27.60.+j

I. INTRODUCTION

Nuclei in the $A \approx$130 region are interesting because they show coexistence of different nuclear shapes. Theoretical calculations predict that, for example, even Ba nuclei are very soft with respect to changes in γ deformation and that they posses a triaxial ($\gamma \approx -30°$) shape in the ground-state band [1,2]. Also, a γ deformation of about $-30°$ is needed in the calculations to reproduce the signature splittings in the neutron $h_{11/2}$ bands in odd-mass Ba nuclei [3,4].

Another interesting property of the even Ba nuclei is that several of them show two S bands, corresponding to proton and neutron $h_{11/2}$ alignments. In the light Ba nuclei with well-deformed shapes, the lower S band is due to the protons [2]. In the heavier Ba isotopes with decreasing quadrupole deformation and more negative γ deformation, the neutron S band becomes favored compared with the proton band. In ^{132}Ba the observed S band has been shown to be of the neutron $h^2_{11/2}$ origin and there is no evidence for the proton alignment [5]. For the nuclei in this mass region, the proton Fermi surface is near the bottom of the $h_{11/2}$ shell, while the neutron Fermi surface is close to the top of the $h_{11/2}$ shell. Therefore, the $h_{11/2}$ protons and neutrons favor prolate ($\gamma \approx 0°$) and oblate ($\gamma \approx -60°$) shapes, respectively.

In the odd-N nuclei, the shape-driving tendency of the $h_{11/2}$ protons results in a strongly coupled character of the neutron $h_{11/2}$ band above the $\pi h^2_{11/2}$ alignment. The $\nu h_{11/2}\pi h^2_{11/2}$ band is an example of bands with intense $M1$ transitions observed in the $A \approx 130$ region [4–9]. At the prolate shape, the neutron $h_{11/2}$ particle is associated with a high K quantum number, while the proton $h_{11/2}$ particle has low K. At the oblate shape, the roles of protons and neutrons are interchanged. In both cases, bands built on the configurations involving $h_{11/2}$ protons and neutrons are expected to show enhanced $M1$ transitions. Systematics of these $M1$ bands has been discussed in [9].

The ^{132}Ba nucleus shows rotational structures [5], while in ^{134}Ba at N = 78 there is little evidence for rotational behavior [10]. For the odd-A nucleus ^{133}Ba the relatively old study of [11] shows the beginning of band structures, although the levels were observed only to $I \sim 12\ \hbar$. The present study of ^{133}Ba was performed by using ^{13}C induced reactions and it was found that band structures persist still up to high spins in ^{133}Ba.

II. EXPERIMENTAL METHODS

The ^{124}Sn(^{13}C,xn)$^{137-x}$Ba reactions at beam energies of 48.4 and 65.5 MeV were used to study high-spin states in the $^{132-134}$Ba nuclei. The 4n-evaporation channel leading to ^{133}Ba nucleus was strong at both bombarding energies. The target consisted of 1.7 mg/cm^2 thick layer of ^{124}Sn enriched to 97.5% on an 11 mg/cm^2 thick gold backing. Results for the ^{132}Ba and ^{134}Ba nuclei will

*Present address: Argonne National Laboratory, Argonne, IL 60439-4843.
†Present address: Laboratoire de Physique Nucléaire, Université de Montréal, C.P. 6128, Montréal, Québec, Canada H3C 3J7.

be reported elsewhere [10,12].

The ^{13}C beams were provided by the Tandem Accelerator Facility at the Niels Bohr Institute. The emitted γ rays were detected in the NORDBALL array [13] consisting of 15 Compton-suppressed Ge detectors and a multiplicity filter of 10 BaF_2 detectors. In order to reduce Coulomb excitation and background activity lines, firing of at least one of the BaF_2 detectors was required in coincidence with at least two Ge detectors. With this trigger condition, slightly over 10^8 $\gamma\gamma$–coincidence events were recorded at both bombarding energies.

The data from the two experiments were separately sorted into two $\gamma\gamma$-coincidence matrices for establishing the level scheme. Sample background-subtracted coincidence spectra are shown in Fig. 1. The NORDBALL array has detectors in four conical rings at 37°, 79°, 101°, and 143° with respect to the beam direction. For deducing information about the transition multipolarities the data were sorted into two E_γ-E_γ matrices with the following angle combinations: (1) (37° + 143°) × all angles and (2) (79° + 101°) × all angles, where first the x axis and then the y axis is given. In this way all the data collected in the experiment could be used for determining the transition multipolarities. By setting equal gates on the y axis on desired γ rays in both matrices coincidence spectra were constructed from which the angular distribution ratios

$$R(E_\gamma) = \frac{I_\gamma(E_\gamma; 37^\circ \text{ or } 143^\circ)}{I_\gamma(E_\gamma; 79^\circ \text{ or } 101^\circ)}$$

were extracted. In each rotational band several gates were set on clean transitions. Note, that the R ratio is independent of the character of the gating transition. For known $\Delta I = 0$ dipole and $\Delta I = 2$ quadrupole transitions this ratio is typically 1.4 – 1.5, while for known stretched dipole transitions it is about 0.80.

III. THE LEVEL SCHEME

The level scheme of ^{133}Ba based on this study is presented in Fig. 2. The observed level structures are organized into the form of nine bands, although a number of states do not belong to these bands. The transitions assigned to ^{133}Ba are collected in Table I together with their intensities and R-ratios. The γ-ray intensities for the lowest transitions in bands 1 and 5 were extracted from the total projection spectrum. For the transitions at higher spins the intensities were obtained from the summed coincidence spectra gated on the bottom transitions of bands 1 and 5.

Band 1 is based on the $1/2^+$ ground state. It was previously known up to the $9/2^+$ state from a β-decay work [14]. Band 5 is built on the 38.9 h $11/2^-$ isomer, which is connected to the $3/2^+$ state of band 1 by a 276.0 keV $M4$ transition [15]. In the present work, we have confirmed the level scheme of [11] for this band up to $I^\pi = 19/2^-$ and further extended it by four new states up to the $27/2^-$ state. The two signatures of band 5 are interconnected by $\Delta I = 1$ transitions having very small R ratios which are consistent with negative values of the multipolarity mixing ratio $\delta(E2/M1)$, see [16] for the

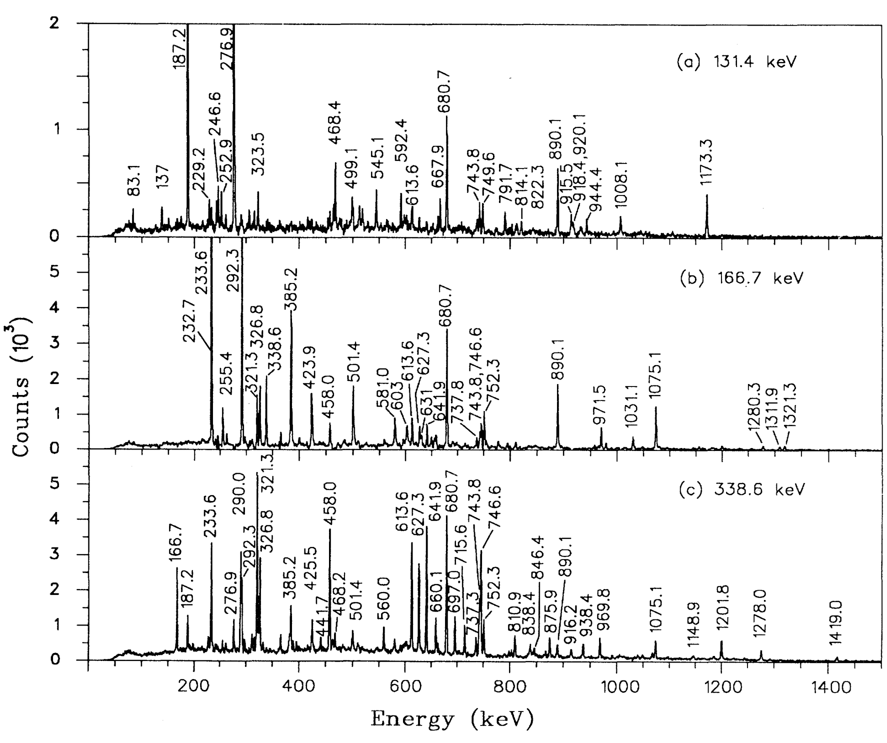

FIG. 1. A sample of coincidence spectra from the $^{124}Sn(^{13}C,4n)^{133}Ba$ reaction at 65.5 MeV bombarding energy.

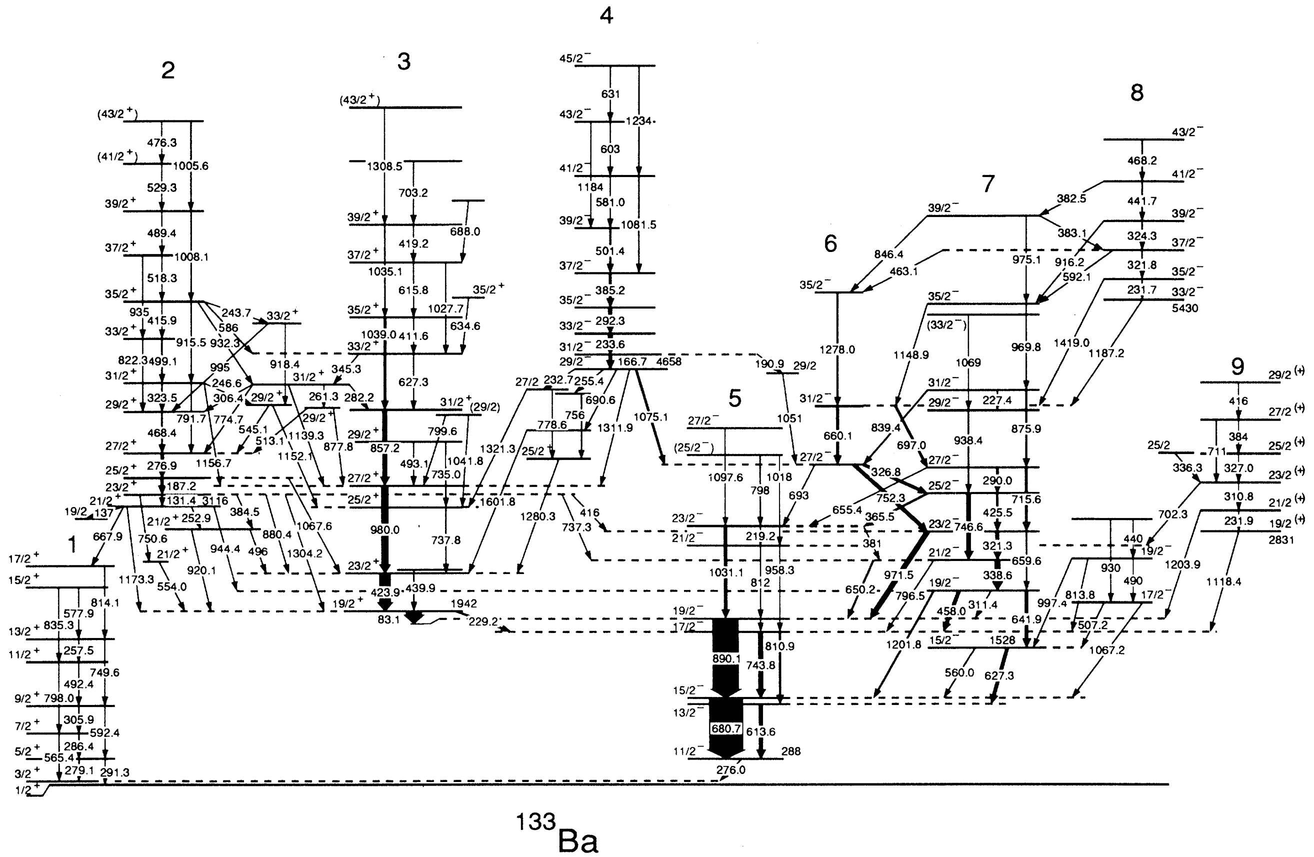

FIG. 2. The level scheme of ^{133}Ba from the present work. The transition energies are given in keV and the widths of the arrows are proportional to the γ-ray intensities.

sign convention of $\delta(E2/M1)$.

The other level structures observed in ^{133}Ba feed through band 5. Only one connection from band 2 to band 1 was established. The band structures 2–4 and 6–9 were previously unknown, except for the few lowest states in bands 3 and 7. Band 3 is built on a $19/2^+$ state at 1942 keV and this irregular band was extended up to the $43/2^+$ state. The 1942 keV state has been reported to have a half-life of 2–5 ns [11]. However, a much longer half-life is indicated by the present data, although lifetimes were not directly extracted. For example, in the coincidence spectrum gated on the 980.0 keV transition, the intensity of the transitions below the $19/2^+$ state is 59% of the 423.9 keV intensity, i.e., part of the intensity is lost due to the narrowness of the coincidence window in the experiment. Comparing with the 52 ns 5^- isomer [17] in ^{134}Ba, it was concluded that the half-life of the bandhead of band 3 is 40 – 50 ns. In Table I, the intensities of the transitions feeding through the 1942 keV isomer are not corrected for this loss of intensity.

Band 2 directly feeds bands 1, 3, and 7, see Fig. 1(a). It is also connected to band 3 via some intermediate states. The spin assignments rely on the facts that the 944.4 and 737.3 keV transitions from band 2 to the $19/2^-$ and $21/2^-$ states in band 7 are of dipole character. The parity of band 2 is fixed to positive by the $E2$ connection to bands 1 and 3.

In band 4 eight intense dipole transitions and three stretched quadrupole transitions were observed, see Fig. 1(b). This band is directly connected to bands 3 and 6. The connecting 1311.9 and 1075.1 keV transitions to the $27/2^+$ and $27/2^-$ states of these bands are of $\Delta I = 1$ character. The R ratio for the 1075.1 keV transition is 0.45(2) which clearly indicates the mixed $M1/E2$ character, while the 1311.9 keV transition has an R ratio of a pure stretched dipole transition. Therefore, the band head of band 4 is assigned to $I^\pi = 29/2^-$.

Band 9 is a sequence of five $\Delta I = 1$ transitions and one crossover $E2$ transition. It is connected to band 5 by three transitions of stretched dipole character. The fact that $\Delta I = 2$ connections to band 5 were not observed might indicate positive parity for this band.

The remaining part of the level scheme consisting of bands 6, 7 and 8 is quite complicated. A coincidence spectrum showing most of the transitions assigned to these structures is given in Fig. 1(c). The two lowest states in band 7 have previously [11] been assigned to $I^\pi = 15/2^-$ and $I^\pi = 19/2^-$. These assignments were confirmed in the present work. Furthermore, we have now constructed band 7 up to $I^\pi = 39/2^-$. Due to many $\Delta I = 2$ connections to band 7, bands 6 and 8 are also assigned negative parity. Characteristic for bands 6 – 8

TABLE I. The γ-ray energies, intensities, and R ratios for the transitions assigned to ^{133}Ba following the ^{124}Sn(^{13}C,4n) reaction.

E_γ[a]	I_γ[b]	R ratio[c]	Spin assignment	Band
83.1	48(5)	1.0(1)	$19/2^+ \to 19/2^-$	3→5
131.4	3.0(2)	0.78(3)	$23/2^+ \to 21/2^+$	2
137	0.23(4)	0.88(7)	$21/2^+ \to 19/2$	2
146.4	0.64(4)	0.87(7)	$19/2^- \to 17/2^-$	5
166.7	9.20(8)	0.82(2)	$31/2^- \to 29/2^-$	4
187.2	7.9(3)	0.80(2)	$25/2^+ \to 23/2^+$	2
190.9	0.6(1)	0.82(8)	$31/2^- \to 29/2$	4→
219.2	0.24(4)	0.47(7)[d]	$23/2^- \to 21/2^-$	5
227.4	1.31(8)	0.93(14)	$31/2^- \to 29/2^-$	7
229.2	5.26(9)	0.93(3)	$19/2^+ \to 17/2^-$	3→5
231.7	0.6(2)		$35/2^- \to 33/2^-$	8
231.9	0.30(4)	0.78(5)[d]	$21/2^{(+)} \to 19/2^{(+)}$	9
232.7	0.9(2)		$29/2^- \to (27/2\ )$	4→
233.6	13.3(5)	0.83(2)	$33/2^- \to 31/2^-$	4
243.7	0.44(4)	0.79(9)	$35/2^+ \to 33/2^+$	2→
246.6	1.00(5)	0.79(3)	$31/2^+ \to 29/2^+$	2→
252.9	0.41(6)	1.76(13)	$21/2^+ \to 21/2^+$	2→
255.4	1.07(6)	0.81(6)	$29/2^- \to 27/2$	4→
257.5	<0.2	0.52(8)[d]	$13/2^+ \to 11/2^+$	1
261.4	0.8(1)	0.63(7)	$31/2^+ \to 29/2^+$	
276.9	6.1(2)	0.80(2)	$27/2^+ \to 25/2^+$	2
279.1	1.9(2)	0.71(3)[d]	$5/2^+ \to 3/2^+$	1
282.2	0.9(1)	1.34(10)	$31/2^+ \to 31/2^+$	→3
286.4	<0.1	1.2(2)[d]	$7/2^+ \to 5/2^+$	1
290.0	7.6(2)	0.76(2)	$27/2^- \to 25/2^-$	7
291.3	0.4(1)	1.43(7)[d]	$5/2^+ \to 1/2^+$	1
292.3	10.8(4)	0.77(2)	$35/2^- \to 33/2^-$	4
305.9	0.22(5)	0.68(4)[d]	$9/2^+ \to 7/2^+$	1
306.4	0.3(1)		$31/2^+ \to 29/2^+$	→2
310.8	0.9(2)	0.85(5)[d]	$23/2^{(+)} \to 21/2^{(+)}$	9
311.4	0.7(2)		$19/2^- \to 19/2^-$	7→5
321.3	11.1(5)	0.74(3)	$23/2^- \to 21/2^-$	7
321.8	1.9(3)		$37/2^- \to 35/2^-$	8
323.5	0.9(1)	0.78(4)	$31/2^+ \to 29/2^+$	2
324.3	1.3(2)	0.56(5)	$39/2^- \to 37/2^-$	8
326.8	8.6(4)	0.74(2)	$27/2^- \to 25/2^-$	6→7
327.0	1.0(2)	0.89(4)[d]	$25/2^{(+)} \to 23/2^{(+)}$	9
336.3	0.20(5)	0.75(10)[d]	$25/2 \to 23/2^{(+)}$	→9
338.6	16.7(6)	0.70(2)	$21/2^- \to 19/2^-$	7
345.3	0.5(2)	0.86(9)	$33/2^+ \to 31/2^+$	3→
365.5	5.3(3)	0.71(3)	$25/2^- \to 23/2^-$	7→5
381	1.6(2)		$23/2^- \to 21/2^-$	5→7
382.5	1.2(3)	0.65(7)[e]	$41/2^- \to 39/2^-$	8→7
383.1	0.8(2)		$39/2^- \to 37/2^-$	7→8
384	0.35(7)	0.81(11)[d]	$27/2^{(+)} \to 25/2^{(+)}$	9
384.5	<0.3	0.77(7)	$23/2^+ \to 21/2^+$	2→
385.2	7.0(3)	0.75(2)	$37/2^- \to 35/2^-$	4
411.6	0.7(1)	0.80(9)	$35/2^+ \to 33/2^+$	3
415.9	0.5(1)	0.75(6)	$35/2^+ \to 33/2^+$	2
416	<0.3		$(29/2\ ) \to 27/2^{(+)}$	9
416	<0.2		$23/2^+ \to 23/2^-$	2→6
419.2	0.67(5)	0.62(8)	$39/2^+ \to 37/2^+$	3
423.9	35.2(10)	1.49(3)	$23/2^+ \to 19/2^+$	3
425.5	5.8(2)	0.50(6)	$25/2^- \to 23/2^-$	7
439.9	0.40(10)		$\to 19/2^+$	3
440	<0.2		$\to 19/2^-$	
441.7	1.7(2)	0.63(5)	$41/2^- \to 39/2^-$	8
458.0	10.5(4)	0.60(2)	$19/2^- \to 17/2^-$	7→5
463.1	1.2(2)	0.67(12)	$37/2^- \to 35/2^-$	8→6
468.2	1.9(3)	0.61(7)	$43/2^- \to 41/2^-$	8
468.4	2.6(2)	0.70(5)	$29/2^+ \to 27/2^+$	2
476.3	0.6(2)		$(43/2^+) \to (41/2^+)$	2
489.4	0.4(1)		$39/2^+ \to 37/2^+$	2
490	0.3(1)		$19/2^- \to 17/2^-$	
492.4	0.15(5)	0.82(13)[d]	$11/2^+ \to 9/2^+$	1
493.1	0.9(1)	0.85(9)	$29/2^+ \to 27/2^+$	3
496	<0.4		$21/2^+ \to 23/2^+$	→3
499.1	2.2(2)	0.76(9)	$33/2^+ \to 31/2^+$	2
501.4	4.2(2)	0.65(3)	$39/2^- \to 37/2^-$	4
507.2	0.5(1)	0.53(5)[d]	$17/2^- \to 15/2^-$	→7
513.1	1.0(1)	0.72(10)	$29/2^+ \to 27/2^+$	→2
518.3	1.3(1)	0.82(10)	$37/2^+ \to 35/2^+$	2
529.3	0.7(1)		$(41/2^+) \to 39/2^+$	2
545.1	1.9(1)	0.72(5)	$29/2^+ \to 27/2^+$	→2
554.0	2.9(2)	0.46(5)	$21/2^+ \to 19/2^+$	→3
560.0	2.6(1)	1.02(7)	$15/2^- \to 15/2^-$	7→5
565.4	0.9(1)	1.34(4)	$7/2^+ \to 3/2^+$	1
577.9	<0.2	0.9(2)[d]	$15/2^+ \to 13/2^+$	1
581.0	2.2(1)	0.62(5)	$41/2^- \to 39/2^-$	4
586	0.3(1)		$35/2^+ \to 33/2^+$	2→3
592.1	1.3(1)	0.65(9)	$37/2^- \to 35/2^-$	8→7
592.4	2.0(1)	1.27(8)	$9/2^+ \to 5/2^+$	1
603	1.0(1)	0.6(2)	$43/2^- \to 41/2^-$	4
613.6	19.0(9)	0.44(2)	$13/2^- \to 11/2^-$	5
615.8	1.3(2)	0.68(10)	$37/2^+ \to 35/2^+$	3
627.3	11.3(5)	0.39(1)	$15/2^- \to 13/2^-$	7→5
627.3	3.6(2)	0.51(4)	$33/2^+ \to 31/2^+$	3
631	0.7(1)	0.6(1)	$45/2^- \to 43/2^-$	4
634.6	1.4(1)	0.55(6)	$35/2^+ \to 33/2^+$	→3
641.9	10.2(5)	1.51(3)	$19/2^- \to 15/2^-$	7
650.2	4.4(2)	0.49(3)	$21/2^- \to 19/2^-$	7→5
655.4	0.7(2)		$27/2^- \to 23/2^-$	7→5
659.6	<1	1.36(8)	$23/2^- \to 19/2^-$	7
660.1	9.0(6)	1.31(12)	$31/2^- \to 27/2^-$	6
667.9	0.9(1)	1.44(8)	$21/2^+ \to 17/2^+$	2→1
680.7	100	1.36(2)	$15/2^- \to 11/2^-$	5
688.0	0.6(1)		$\to 37/2^+$	→3
690.6	0.5(2)		$29/2 \to$	4→
693	1.0(3)		$27/2^- \to 23/2^-$	6→5
697.0	6.4(5)	1.35(7)	$31/2^- \to 27/2^-$	6→7
702.3	0.5(1)	0.9(1)[d]	$23/2^{(+)} \to 21/2^-$	9→5
703.2	0.7(2)		$\to 39/2^+$	3
711	<0.2		$27/2^{(+)} \to 23/2^{(+)}$	9
715.6	7.6(3)	1.42(8)	$27/2^- \to 23/2^-$	7
735.0	0.4(1)		$29/2^+ \to 25/2^+$	3
737.3	1.8(1)	0.74(5)	$23/2^+ \to 21/2^-$	2→7
737.8	4.0(2)	0.36(2)	$25/2^+ \to 23/2^+$	3
743.8	14.9(5)	0.48(2)	$17/2^- \to 15/2^-$	5
746.6	12.4(4)	1.45(4)	$25/2^- \to 21/2^-$	7
749.6	2.1(2)	1.31(5)	$13/2^+ \to 9/2^+$	1
750.6	0.8(2)		$23/2^+ \to 21/2^+$	2→
752.3	10.5(3)	1.45(4)	$27/2^- \to 23/2^-$	6→7
756	<0.3		$27/2 \to 25/2^+$	
774.7	0.5(1)	1.22(11)	$31/2^+ \to 27/2^+$	→2
778.6	0.5(1)	0.74(7)	$(27/2) \to 25/2^+$	
791.7	1.4(1)	1.39(8)	$31/2^+ \to 27/2^+$	2

TABLE I. (*Continued*).

E_γ [a]	I_γ [b]	R ratio [c]	Spin assignment	Band
796.5	1.5(1)	1.4(2)	$21/2^- \to 17/2^-$	7→5
798.0	0.8(1)	1.26(8) [d]	$11/2^+ \to 7/2^+$	1
798	<0.3		$(25/2^-) \to 23/2^-$	5
799.6	0.5(2)		$(29/2) \to 27/2^+$	→3
810.9	6.5(2)	1.33(7)	$17/2^- \to 13/2^-$	5
812	1.6(3)	0.58(6)	$21/2^- \to 19/2^-$	5
813.8	0.5(1)	0.48(5) [d]	$19/2^- \to 17/2^-$	→5
814.1	1.0(1)	1.32(8)	$17/2^+ \to 13/2^+$	1
822.3	0.4(1)	1.5(3)	$33/2^+ \to 29/2^+$	2
835.3	0.35(6)	1.26(7) [d]	$15/2^+ \to 11/2^+$	1
839.4	3.0(2)	1.45(12)	$31/2^- \to 27/2^-$	7→6
846.4	1.2(3)	1.33(10)	$39/2^- \to 35/2^-$	7→6
857.2	14.3(4)	1.43(2)	$31/2^+ \to 27/2^+$	3
875.9	5.4(2)	1.5(2)	$31/2^- \to 27/2^-$	7
877.8	0.9(2)	1.22(10)	$29/2^+ \to 27/2^+$	→3
880.4	1.6(2)	1.29(8)	$23/2^+ \to 23/2^+$	2 →3
890.1	78(2)	1.36(4)	$19/2^- \to 15/2^-$	5
915.5	2.0(1)	1.46(9)	$35/2^+ \to 31/2^+$	2
916.2	2.6(2)	1.32(14)	$39/2^- \to 35/2^-$	8→7
918.4	0.8(1)	1.4(2)	$33/2^+ \to 29/2^+$	
920.1	0.5(1)	0.59(13)	$21/2^+ \to 19/2^+$	→3
930	<0.3		$\to 17/2^-$	
932.3	0.8(1)	1.4(2)	$35/2^+ \to 31/2^+$	2→
935	0.6(1)		$37/2^+ \to 33/2^+$	2
938.4	3.0(2)	1.42(10)	$29/2^- \to 25/2^-$	7
944.4	0.9(1)	0.81(7)	$21/2^+ \to 19/2^-$	2→7
958.3	1.6(1)	1.4(2)	$21/2^- \to 17/2^-$	5
969.8	5.4(4)	1.30(10)	$35/2^- \to 31/2^-$	7
971.5	14.7(5)	1.23(6)	$23/2^- \to 19/2^-$	7→5
975.1	0.5(1)		$39/2^- \to 35/2^-$	7
980.0	21.1(8)	1.44(3)	$27/2^+ \to 23/2^+$	3
995	0.2(1)		$33/2^+ \to 29/2^+$	→2
997.4	0.2(1)	1.3(2) [d]	$19/2^- \to 15/2^-$	→7
1005.6	0.6(1)		$(43/2^+) \to 39/2^+$	2
1008.1	2.1(2)	1.42(9)	$39/2^+ \to 35/2^+$	2
1018	0.3(1)		$(25/2^-) \to 21/2^-$	5
1027.7	0.6(1)	1.2(2)	$37/2^+ \to 33/2^+$	3
1031.1	8.8(6)	1.41(4)	$23/2^- \to 19/2^-$	5
1035.1	2.2(1)	1.36(7)	$39/2^+ \to 35/2^+$	3
1039.0	6.0(3)	1.29(6)	$35/2^+ \to 31/2^+$	3
1041.8	0.9(1)	1.26(10)	$(29/2^+) \to 25/2^+$	→3
1051	0.7(2)		$29/2 \to 27/2^-$	→6
1067.2	<1	0.45(5) [d]	$17/2^- \to 15/2^-$	→5
1067.6	1.3(1)	0.65(6)	$25/2^+ \to 23/2^+$	2→3
1069	0.9(2)		$(33/2^-) \to 29/2^-$	7
1075.1	6.0(3)	0.45(2)	$29/2^- \to 27/2^-$	4→6
1081.5	0.3(1)	1.4(2)	$41/2^- \to 37/2^-$	4
1097.6	1.2(1)	1.8(2)	$27/2^- \to 23/2^-$	5
1118.4	0.5(1)	0.80(6) [d]	$19/2^{(+)} \to 17/2^-$	9→5
1139.3	1.4(1)	1.58(14)	$31/2^+ \to 27/2^+$	→3
1148.9	0.9(1)	1.7(2)	$35/2^- \to 31/2^-$	7→6
1152.1	0.4(1)		$29/2^+ \to 25/2^+$	→3
1156.7	0.9(1)		$31/2^+ \to 27/2^+$	2→3
1173.3	2.4(1)	0.67(6)	$21/2^+ \to 19/2^+$	2→3
1184	0.3(1)		$43/2^- \to 39/2^-$	4
1187.2	1.8(1)	0.51(7)	$33/2^- \to 31/2^-$	8→6
1201.8	4.3(2)	1.56(13)	$19/2^- \to 15/2^-$	7→5
1203.9	1.6(1)	0.87(7)	$21/2^{(+)} \to 19/2^-$	9→5
1234	<0.2		$45/2^- \to 41/2^-$	4
1278.0	4.4(2)	1.38(10)	$35/2^- \to 31/2^-$	6
1280.3	1.2(1)	0.59(6)	$25/2^+ \to 23/2^+$	→3
1304.2	0.9(2)	1.29(15)	$23/2^+ \to 19/2^+$	2→3
1308.5	0.5(1)		$(43/2^+) \to 39/2^+$	3
1311.9	0.6(1)	0.80(9)	$29/2^- \to 27/2^+$	4→3
1321.3	0.6(1)	0.94(11)	$(27/2) \to 25/2^+$	→3
1419.0	2.1(1)	1.35(14)	$35/2^- \to 31/2^-$	8→6
1601.8	0.4(1)		$\to 23/2^+$	→3

[a] Transition energies given with a decimal are accurate to 0.1 keV, otherwise accurate to 0.5 keV.
[b] Intensities from the data taken at 65.5 MeV.
[c] R ratios extracted in most cases from the 65.5 MeV data.
[d] R ratio extracted from the 48.4 MeV data.
[e] R ratio is that of the 382.5 – 383.1 keV doublet.

is that the $\Delta I = 1$ transitions have small R ratios indicating a negative sign for the multipolarity mixing ratio.

IV. DISCUSSION

Our experiments on ^{133}Ba have established many new bands, which provide information for probing its microscopic structure. Most of these bands show both signatures connected by $\Delta I = 1$ transitions. A characteristic feature is also that the bands are in many cases irregular and perhaps strongly mixed. Rotational properties of the observed bands are interpreted below in terms of the cranked shell model (CSM) [18]. To compare our experimental results with the CSM predictions the experimental data have been expressed in the rotating frame of reference. A reference given by the Harris parameters $J_0 = 10\hbar^2/\text{MeV}$ and $J_1 = 20\hbar^4/\text{MeV}^3$ has been used to describe the energy of the rotating core. The values of the Harris parameters were chosen so that the yrast sequence in ^{132}Ba [5] showed an alignment around $0\hbar$ at low spins and a constant alignment of about $7\hbar$ above the first band crossing. Plots for Routhians e' and aligned angular momenta i_x are presented in Fig. 3. Discussions of quasiparticle configurations and alignments, as well as comparisons with the results of the total Routhian surface (TRS) calculations [19] are given below.

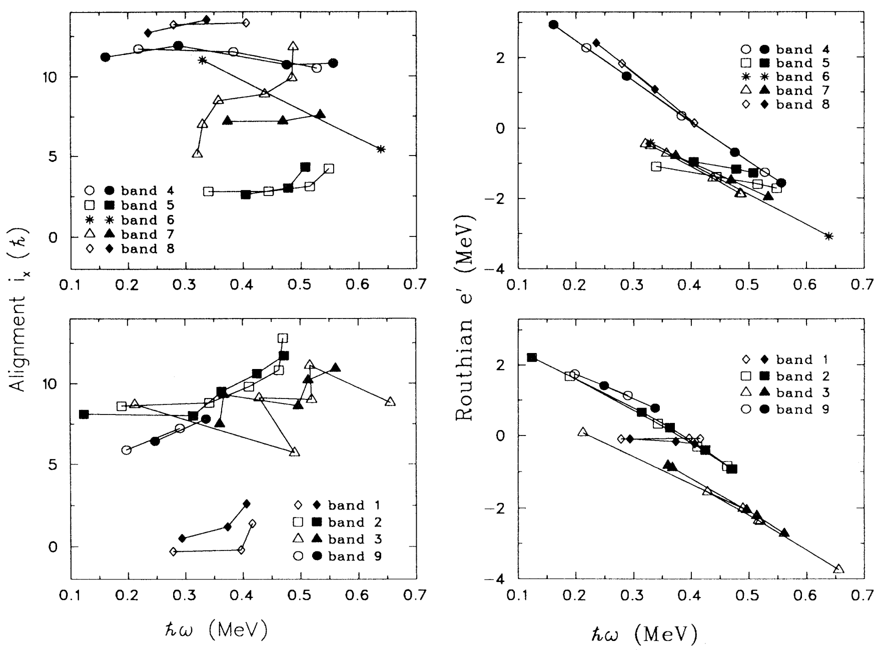

FIG. 3. Experimental alignments and Routhians for bands in ^{133}Ba. A reference describing the energy of the rotating core has been subtracted. Open and closed symbols correspond to the $\alpha = -1/2$ and $\alpha = 1/2$ signatures, respectively. The following values of the K quantum number were used: K = 0.5 for bands 1, 3, 5–7; $K = 7.5$ for bands 2 and 9; and $K = 8.5$ for bands 4 and 8.

A. Bands built on the one-quasiparticle states

Band 5 is built on an orbital from the $h_{11/2}$ shell. For the neutron number $N = 77$ and a prolate deformation the $\Omega = 11/2$ component is expected to be close to the Fermi surface, resulting in a band structure with insignificant signature splitting. In contrast, band 5 shows a signature splitting of about 300 keV, similar as in the ^{135}Ce isotone [8]. Large signature splittings have also been observed in the other neighboring odd-N nuclei [4,6]. These large signature splittings have been attributed to a triaxial shape with $\gamma \approx$ -30° [6,8]. To account for the observed signature splitting in ^{133}Ba by standard CSM calculation, one has to assume $\gamma \approx -40°$ or $\gamma \approx -90°$.

The bands built on the $1/2^+$ ground states in the ^{129,131}Ba isotopes have been interpreted to arise from a mixed $s_{1/2}/d_{3/2}$ configuration [4,6]. In ^{133}Ba, the $3/2^+$ state of band 1 is only 12 keV higher in energy than the $1/2^+$ ground state, indicating the $d_{3/2}$ configuration. However, the experimental $B(M1)/B(E2)$ ratios shown in Fig. 4 are larger than the $d_{3/2}$ estimates obtained by using a geometrical model [20,21]. Also, one would expect the $\alpha = -1/2$ signature to be favored over the $\alpha = 1/2$ signature in a $d_{3/2}$ band, while the observed band shows an opposite trend. An $s_{1/2}$ admixture in the configuration might explain these findings.

Results of the TRS calculations are shown in Fig. 5. In general, these calculations predict very soft surfaces for ^{133}Ba. The surfaces extracted for the negative parity states show minima around $\beta_2 = 0.12$, $\gamma \approx -75°$ and $\beta_2 = 0.12$, $\gamma \approx -90°$ in the $\alpha = -1/2$ and $\alpha = 1/2$ signatures, respectively. The calculated signature splitting is about 400 keV, which is slightly larger than the experimental value. At low rotational frequencies, the TR

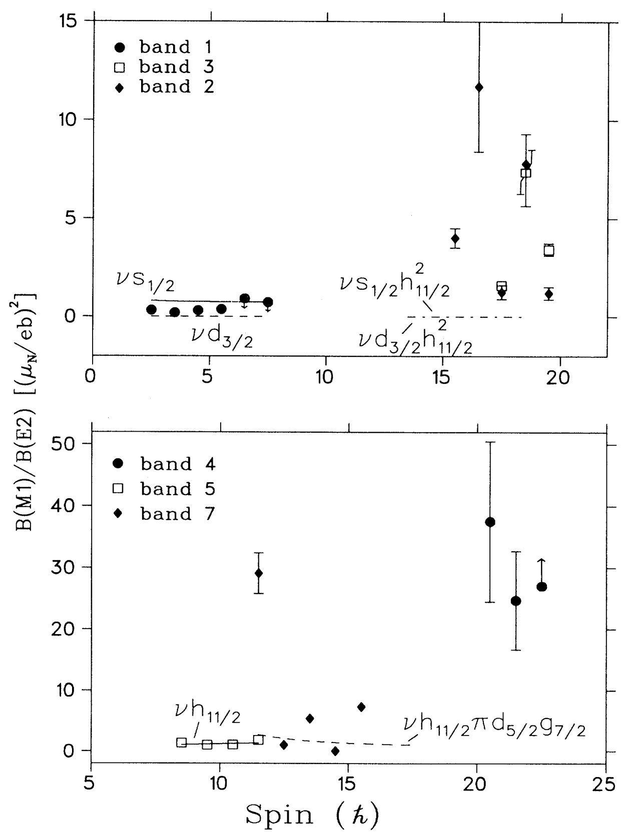

FIG. 4. Experimental and theoretical $B(M1)/B(E2)$ ratios for some bands in ^{133}Ba. In the theoretical calculations a quadrupole moment of $Q_0 = 2$ e b was assumed. The calculated ratios for the $\nu s_{1/2}h^2_{11/2}$ and $\nu d_{3/2}h^2_{11/2}$ configurations are very small and fall therefore on the same line.

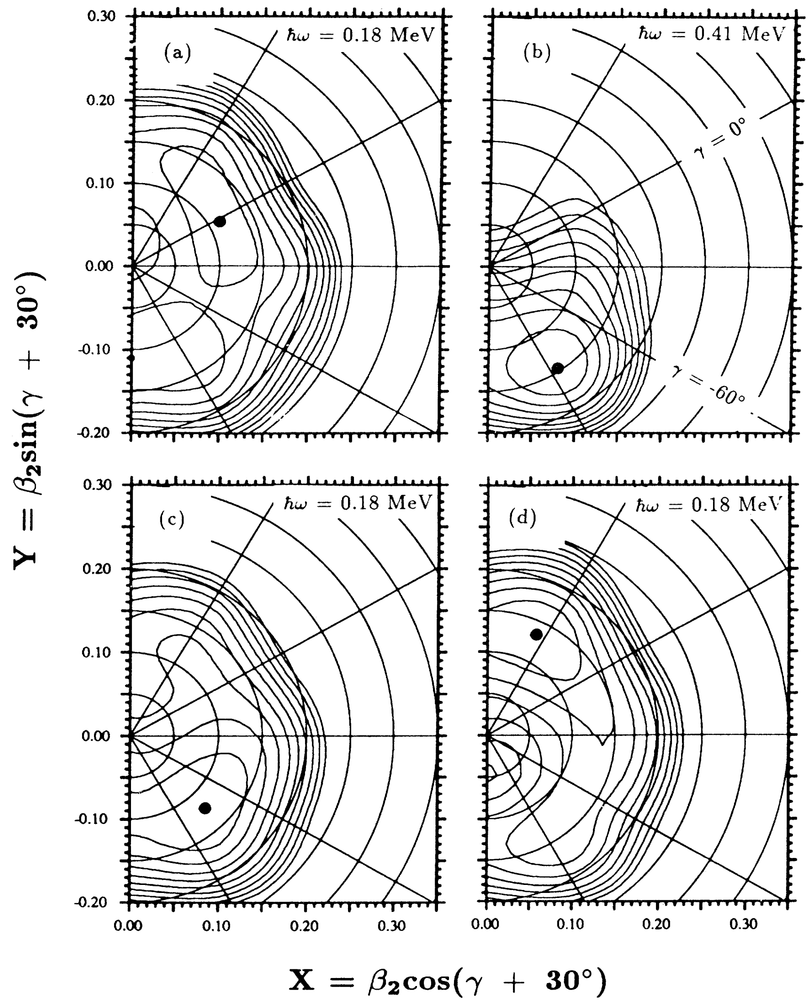

FIG. 5. Total Routhian surfaces in ^{133}Ba. (a) and (b) show the lowest neutron $(\pi, \alpha) = (+, -1/2)$ configuration, (c) the lowest neutron $(-, -1/2)$ configuration, and (d) the lowest $(-, -1/2)_n(-, -1/2)_p(+, -1/2)_p$ configuration.

surfaces for the lowest positive parity configurations show very shallow minima between $\beta_2 = 0.10$ and $\beta_2 = 0.15$, and $\gamma = -30°$ and $\gamma = 30°$.

B. Multiquasiparticle bands

Band 3 is an irregular band built on a low-lying isomeric $19/2^+$ state. Such $19/2^+$ isomers have been also observed in the $N = 77$ isotones ^{131}Xe [22] and ^{135}Ce [8] and have been associated with the neutron $\nu s_{1/2}h_{11/2}^2$ configuration. In ^{135}Ce the configuration assignment is also confirmed by a g-factor measurement [23]. For this three-quasiparticle configuration, states with $I = 19/2$ and $I = 21/2$ are expected. In the shell model, the two-nucleon interaction in the $\nu s_{1/2}h_{11/2}$ configuration is about 250 keV more attractive for the 5^- state than for the 6^- state. Thus in the three-quasiparticle $\nu s_{1/2}h_{11/2}^2$ configuration the $19/2^+$ state should be found at lower energy than the $21/2^+$ state. Contrary to the above $N = 77$ nuclei, an $\alpha = 1/2$ band in ^{131}Ba starting at $I = 21/2$ and 2.616 MeV excitation energy has been associated with the $\nu s_{1/2}h_{11/2}^2$ configuration [6].

The $23/2^+$ state of band 3 is quite close to the bandhead. Since the $\nu d_{3/2}$ quasiparticle state is very close to the $\nu s_{1/2}$ state, the $23/2^+$ state of band 3 and the band on top of it can perhaps be associated with the $\nu d_{3/2}h_{11/2}^2$ configuration. The $19/2^+$ and $23/2^+$ states are also related to the lowest 5^- and 7^- states in neighboring even-mass nuclei. In Fig. 6 these states are shown for $^{130-132}$Xe [22,24] and $^{132-134}$Ba [11,17]. The 5^- and 7^- states are 174–363 keV apart and have been interpreted as arising from the $\nu s_{1/2}h_{11/2}$ and $\nu d_{3/2}h_{11/2}$ configurations, respectively.

In ^{133}Ba the crossing of bands 1 and 3 occurs at $\hbar\omega \approx 0.24$ MeV with an alignment gain of about $8\hbar$ (assuming $K = 1/2$ for both bands). At higher spin the alignment and Routhian plots reveal irregularities with small alignment gains. Near the bandhead band 3 is of decoupled character. Above $I = 31/2$ the level pattern develops towards that of a strongly coupled band. The experimental $B(M1)/B(E2)$ ratios (see Fig. 4) are much larger than the theoretical estimates for the $s_{1/2}h_{11/2}^2$ and $d_{3/2}h_{11/2}^2$ configurations, which also suggests a change in the configuration. To account for the experimental $B(M1)/B(E2)$ ratios, a configuration involving both

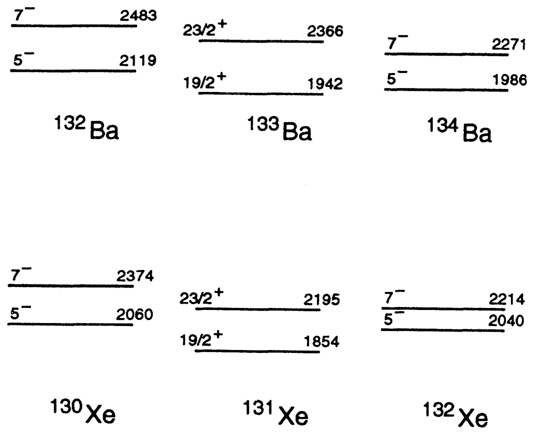

FIG. 6. Systematics of the lowest 5^-, 7^- states in the even nuclei and $19/2^+$, $23/2^+$ states in the odd-N nuclei around ^{133}Ba.

protons and neutrons is needed.

In the TR surfaces for the lowest positive parity configuration the neutron $h_{11/2}$ alignment takes place around the frequency of 0.22 MeV, in good agreement with the experimental crossing frequency of bands 1 and 3. The $h_{11/2}$ alignment drives the nuclear shape to a large negative value of γ, as shown in Fig. 5. The $\alpha = -1/2$ sequence is calculated to be clearly favored compared with the $\alpha = 1/2$ sequence, also in accord with the level scheme and the proposed $d_{3/2}h_{11/2}^2$ configuration. It is interesting to note that in the TR surfaces the minimum at $\beta_2 \approx 0.145$, $\gamma \approx -85°$ persists up to the frequency of about 0.50 MeV, i.e., roughly to the frequency where the change in the level pattern is observed.

Band 2 starts with intense $\Delta I = 1$ transitions, while at higher spin also $\Delta I = 2$ transitions are observed. The extracted $B(M1)/B(E2)$ ratios (cf. Fig. 4) are quite large and show a pronounced staggering. This band we associate with the $\nu h_{11/2}\pi h_{11/2}g_{7/2}$ configuration, following the configuration assignments of similar bands in the neighboring odd-N nuclei [6,8]. The configuration assignment is further supported by a comparison with ^{132}Ba: The bandhead of band 2 lies about 2.8 MeV above the $11/2^-$ state of the $h_{11/2}$ band, which is not so far from the excitation energy of the $\pi h_{11/2}g_{7/2}$ 9^- state in ^{132}Ba [5]. Inspection of Fig. 3 reveals that band 2 has $(8\text{–}9)\hbar$ aligned angular momentum, which is similar to that of the $\pi h_{11/2}g_{7/2}$ band in ^{132}Ba. We also note that the $\alpha = -1/2$ signature is slightly lower in energy than the $\alpha = 1/2$ signature. As pointed out in [6], the $\alpha = -1/2$ signature of the $\nu h_{11/2}\pi h_{11/2}g_{7/2}$ band should be energetically favored when $\gamma > 10°$. Indeed, a minimum around $\beta_2 \approx 0.13$, $\gamma \approx 35°$ is seen in the TR surfaces [see Fig. 5(d)].

Bands 4, 8, and 9 are regular bands composed of intense $\Delta I = 1$ transitions. Bands 8 and 9 are nonyrast and only weakly populated in the present reaction, whereas band 4 receives a considerable fraction of the intensity. Band 4 becomes actually yrast around $I = 41/2$. Similar bands have also been observed in many neighboring nuclei. One such $\Delta I = 1$ band, observed in the neighboring odd-N nuclei, is built on the $\nu h_{11/2}\pi h_{11/2}^2$ configuration. In ^{131}Ba and ^{135}Ce this band is connected to the one-quasiparticle $h_{11/2}$ band mainly by $\Delta I = 2$ transitions [6,8]. In these nuclei, the proton $h_{11/2}$ alignment takes place in the frequency range of 0.40 – 0.45 MeV. Among the strongly coupled bands observed in ^{133}Ba only band 9 is directly connected to the neutron $h_{11/2}$ band. However, the connecting transitions are of $\Delta I = 1$ type and the bandhead spin is $I = 19/2$, compared to $I = 27/2$ for the $\nu h_{11/2}\pi h_{11/2}^2$ band in ^{131}Ba and ^{135}Ce. The aligned angular momenta and Routhians extracted for band 9 are quite similar to those for band 2. Therefore, it is proposed that band 9 is built on a similar configuration as band 2, e.g., the $\nu h_{11/2}\pi h_{11/2}d_{5/2}$ configuration at a prolate shape.

Since bands 4 and 8 start at high excitation energies, they are most likely built on five-quasiparticle configurations. A band similar to band 4 has been reported in ^{135}Ce [8]. Its $I = 27/2$ bandhead is at 4.496 MeV, while in band 4 the $I = 29/2$ bandhead is at 4.658 MeV. There is a similar band also in ^{132}Ba with a 14^- bandhead at 5.721 MeV [12]. The band in ^{135}Ce has been associated with the oblate $\nu s_{1/2}h_{11/2}^2\pi h_{11/2}g_{7/2}$ configuration. The bandhead of band 4 lies about 2.7 MeV above the bandhead of band 3, compared to about 2.8 MeV between bands 2 and 5. In both cases, the difference in the configurations is the same, i.e., proton $h_{11/2}g_{7/2}$. Although shape changes are also involved, it seems to be possible to associate band 4 with the configuration earlier suggested for the similar band in ^{135}Ce. The alignment extracted for band 4 is shown in Fig. 3. The K value of 17/2 used is comprised of $K = 11/2$ for the proton $h_{11/2}$, $K = 5/2$ for the proton $g_{7/2}$, and $K = 1/2$ for the neutron $s_{1/2}$ configuration. The $B(M1)/B(E2)$ ratios measured in this band are 10–20 times larger than in band 5 and also clearly larger than in band 2 built on the prolate $\nu h_{11/2}\pi h_{11/2}g_{7/2}$ configuration. Both the large aligned angular momentum and large $B(M1)/B(E2)$ ratios are consistent with the proposed five-quasiparticle configuration. Band 8 is associated with slightly larger alignment than band 4. In the Routhian plot band 8 lies 200–300 keV higher than band 4. Band 8 might be built on a similar configuration as band 4.

In addition to the strongly coupled structures, also decoupled sequences have been observed in the neighboring odd-N nuclei [6,8]. Some of these sequences have been interpreted to arise from the $\nu h_{11/2}^3$ configuration possessing nearly an oblate ($\gamma = -60°$) shape. Such a band is also predicted in ^{133}Ba. In the TR surfaces, the crossing between the $\nu h_{11/2}^3$ and the $\nu h_{11/2}$ bands occurs at $\hbar\omega \approx 0.33$ MeV. Due to the large negative value of γ ($\approx -80°$), this configuration is expected to show a large signature splitting. Above $I = 19/2$, both signatures are observed in band 7 and the signature splitting is not as large as the TR surfaces indicate for the $\nu h_{11/2}^3$ band. Therefore, band 7 is not likely to be built on this configuration. Instead, band 6 might arise from this configuration.

The properties of band 7 vary considerably with spin. There are large changes in the $B(M1)/B(E2)$ ratios and the $\alpha = -1/2$ signature shows a clear alignment gain at low rotational frequencies, suggesting a configuration change around $I = 21/2$. The $15/2^-$ and $19/2^-$ states can perhaps be understood as a consequence of the γ vibration built on the neutron $h_{11/2}$ configuration. Note, that the γ band of ^{132}Ba is rather irregular with a low-lying 6^+ state [5], which might have a dominant $\pi d_{5/2}g_{7/2}$ configuration [24]. It is proposed that the upper part of band 7 is built on the $\nu h_{11/2}\pi d_{5/2}g_{7/2}$ configuration. The prolate $\nu s_{1/2}\pi h_{11/2}g_{7/2}$ or $\nu d_{3/2}\pi h_{11/2}d_{5/2}$ configurations can also account for the observed alignment and the signature splittings at higher spin, but not likely for the large experimental $B(M1)/B(E2)$ ratios.

V. SUMMARY

Excited states of ^{133}Ba have been studied using ^{13}C induced reactions and the NORDBALL detector array. It was found that bandlike structures persist still in ^{133}Ba. In total, nine bands were observed. Most of the bands show intense $M1$ transitions. By comparing the band properties with known bands in neighboring nuclei, configuration assignments have been made. The one-quasiparticle neutron $h_{11/2}$ band is associated with large signature splitting. In the TR surfaces this band has a minimum at very large negative γ deformation, $\gamma \approx -80°$. Multiquasiparticle bands built on pure neutron as well as on mixed proton-neutron configurations were also identified. The latter kind of configurations may posses either $\gamma > 0°$ or $\gamma < -60°$, depending on the number of $h_{11/2}$ protons and neutrons involved.

ACKNOWLEDGMENTS

This work was partially supported by the Academy of Finland, Danish Natural Science Research Council, Swedish Natural Science Research Council, and the NORDBALL Collaboration. We are grateful to the staff of the Tandem Accelerator Laboratory at NBI for providing excellent beams and technical support.

[1] I. Ragnarsson, A. Sobiczewski, R. K. Sheline, S. E. Larsson, and B. Nerlo-Pomorska, Nucl. Phys. **A233**, 329 (1974)

[2] R. Wyss, A. Granderath, R. Bengtsson, P. von Brentano, A. Dewald, A. Gelberg, A. Gizon, J. Gizon, S. Harrissopulos, A. Johnson, W. Lieberz, W. Nazarewicz, J. Nyberg and K. Schiffer, Nucl. Phys. **A505**, 337 (1989).

[3] J. Gizon, A. Gizon, and J. Meyer-ter-Vehn, Nucl. Phys. **A277**, 464 (1977).

[4] A. P. Byrne, K. Schiffer, G. D. Dracoulis, B. Fabricius, T. Kibédi, A. E. Stuchbery, and K. B. Lieb, Nucl. Phys. **A548**, 131 (1992).

[5] E. S. Paul, D. B. Fossan, Y. Liang, R. Ma, and N. Xu, Phys. Rev. C **40**, 1255 (1989).

[6] R. Ma, Y. Liang, E. S. Paul, N. Xu, D. B. Fossan, L. Hildingsson, and R. Wyss, Phys. Rev. C **41**, 717 (1990).

[7] L. Hildingsson, C. W. Beausang, D. B. Fossan, R. Ma, E. S. Paul, W. F. Piel, Jr., and N. Xu, Phys. Rev. C **39**, 471 (1989).

[8] R. Ma, E. S. Paul, D. B. Fossan, Y. Liang, N. Xu, R. Wadsworth, I. Jenkins, and P. J. Nolan, Phys. Rev. C **41**, 2624 (1990).

[9] E. S. Paul, D. B. Fossan, Y. Liang, R. Ma, N. Xu, R. Wadsworth, I. Jenkins, and P. J. Nolan, Phys. Rev. C **41**, 1576 (1990).

[10] T. Lönnroth, P. Ahonen, C. Fahlander, R. Julin, S. Juutinen, K.-M. Källman, A. Lampinen, P. Manngård, J. Nyberg, A. Pakkanen, K. Schiffer, G. Sletten, S. Törmänen, A. Virtanen and R. Wyss, unpublished.

[11] J. Gizon, A. Gizon, and D. J. Horen, Nucl. Phys. **A252**, 509 (1975).

[12] S. Juutinen, S. Törmänen, P. Ahonen, M. Carpenter, C. Fahlander, J. Gascon, R. Julin, A. Lampinen, T. Lönnroth, J. Nyberg, A. Pakkanen, M. Piiparinen, K. Schiffer, P. Simezek, G. Sletten, and A. Virtanen, unpublished.

[13] B. Herskind, Nucl. Phys. **A447**, 385c (1985); G. Sletten, J. Gascon, and J. Nyberg, Proceedings of the International Conference on the Spectroscopy of Heavy Nuclei, Crete, Greece, 1989 [Int. Phys. Conf. Ser. 105, 125 (1990)].

[14] E. A. Henry and R. A. Meyer, Phys. Rev. C **13**, 2501 (1976).

[15] J. E. Thun, S. Törnkvist, F. Falk, and H. Snellman, Nucl. Phys. **67**, 625 (1965).

[16] E. der Mateosian and A. W. Sunyar, At. Data Nucl. Data Tables **13**, 407 (1974).

[17] T. Morek, H. Beuscher, B. Bochev, D. R. Haenni, R. M. Lieder, T. Kutsarova, M. Müller-Veggian, and A. Neskakis, Z. Phys. A **298**, 267 (1980).

[18] R. Bengtsson and S. Frauendorf, Nucl. Phys. **A327**, 139 (1979).

[19] R. Wyss, J. Nyberg, A. Johnson, R. Bengtsson, and W. Nazarewicz, Phys. Lett. B **215**, 211 (1988).

[20] F. Dönau and S. Frauendorf, in *Proceedings of the Conference on High Angular Momentum Properties of Nuclei, Oak Ridge, 1982,* edited by N. R. Johnson (Harwood-Academic, New York, 1983), p. 143; F. Dönau, Nucl. Phys. **A471**, 469 (1987).

[21] D. C. Radford, H. R. Andrews, G. C. Ball, D. Horn, D. Ward, F. Banville, S. Flibotte, S. Monaro, S. Pilotte, P. Taras, J. K. Johansson, D. Tucker, J. C. Waddington, M. A. Riley, G. B. Hagemann, and I. Hamamoto, Nucl. Phys. **A545**, 665 (1992).

[22] A. Kerek, A. Luukko, M. Grecescu, and J. Sztarkier, Nucl. Phys. **A172**, 603 (1971).

[23] A. Zemel, C. Broude, E. Dafni, A. Gelberg, M. B. Goldberg, J. Gerber, G. J. Kumbartzki, and K.-H. Speidel, Z. Phys. A **304**, 269 (1982).

[24] T. Lönnroth, J. Hattula, H. Helppi, S. Juutinen, K. Honkanen, and A. Kerek, Nucl. Phys. **A431**, 256 (1984).